environmental microbiology

Environmental Microbiology (2019) **21**(8), 2659–2676 doi:10.1111/1462-2920.14577

Transcriptomics analysis defines global cellular response of *Agrobacterium tumefaciens* 5A to arsenite exposure regulated through the histidine kinases PhoR and AioS

Rachel A. Rawle,[1] Yoon-Suk Kang,[2†] Brian Bothner,[3] Gejiao Wang [4] and Timothy R. McDermott [2*]

[1]*Department of Microbiology and Immunology, Montana State University, Bozeman, MT 59717, USA.*

[2]*Department of Land Resources and Environmental Sciences, Montana State University, Bozeman, MT 59717, USA.*

[3]*Department of Chemistry and Biochemistry, Montana State University, Bozeman, MT 59717, USA.*

[4]*State Key Laboratory of Agricultural Microbiology, College of Life Science and Technology, Huazhong Agricultural University, Wuhan 430070, China.*

Summary

In environments where arsenic and microbes coexist, microbes are the principal drivers of arsenic speciation, which directly affects bioavailability, toxicity and bioaccumulation. Speciation reactions influence arsenic behaviour in environmental systems, directly affecting human and agricultural exposures. Arsenite oxidation decreases arsenic toxicity and mobility in the environment, and therefore understanding its regulation and overall influence on cellular metabolism is of significant interest. The arsenite oxidase (AioBA) is regulated by a three-component signal transduction system AioXSR, which is in turn regulated by the phosphate stress response, with PhoR acting as the master regulator. Using RNA-sequencing, we characterized the global effects of arsenite on gene expression in *Agrobacterium tumefaciens* 5A. To further elucidate regulatory controls, mutant strains for histidine kinases PhoR and AioS were employed, and illustrate that in addition to arsenic metabolism, a host of other functional responses are regulated in parallel. Impacted functions include arsenic and phosphate metabolism, carbohydrate metabolism, solute transport systems and iron metabolism, in addition to others. These findings contribute significantly to the current understanding of the metabolic impact and genetic circuitry involved during arsenite exposure in bacteria. This informs how arsenic contamination will impact microbial activities involving several biogeochemical cycles in nature.

Received 8 November, 2018; revised 28 January, 2019; accepted 26 February, 2019. *For correspondence. E-mail timmcder@exchange.montana.edu; Fax 406-994-3933. †Present address: Department of Pathology, Beth Israel Deaconess Medical Center, Harvard Medical School, Boston, MA 02215, USA.

Introduction

Arsenic is the most common elemental toxin in water and soil systems across the world and has been the highest priority EPA contaminant for over a decade (*Agency for Toxic Substances and Disease Registry*, 2017). An estimated 250 million people worldwide have been exposed to excessive levels of arsenic, which over the long-term leads to a variety of diseases and cancers (Kapaj *et al*., 2006; Naujokas *et al*., 2013). Important factors affecting arsenic cycling in the environment and human exposure (i.e. toxicity, bioavailability and bioaccumulation) are directly related to its chemical speciation (Inskeep *et al*., 2001). In every environment where arsenic and microbes coexist, microbes are principal drivers of this chemical speciation, and are thus an integral part of understanding arsenic cycling (Kang *et al*., 2012a).

A critical arsenic transformation process occurring in nature is arsenite (As^{III}) oxidation. As^{III}-oxidizing microorganisms may utilize As^{III} as a sole electron donor, deriving energy from the oxidation of As^{III} to arsenate (As^{V}). As^{III} oxidation can also be a detoxification mechanism, converting the more toxic As^{III} to the less toxic As^{V}. The soil bacterium *Agrobacterium tumefaciens* 5A is a model organism for As^{III} oxidation, and studies during the past decade involving this organism have yielded several important observations about the cellular mechanisms that control As^{III} oxidation. First, the sensing of As^{III} and induction of the As^{III} oxidase occurs through a three-component signal transduction system (Kashyap *et al*.,

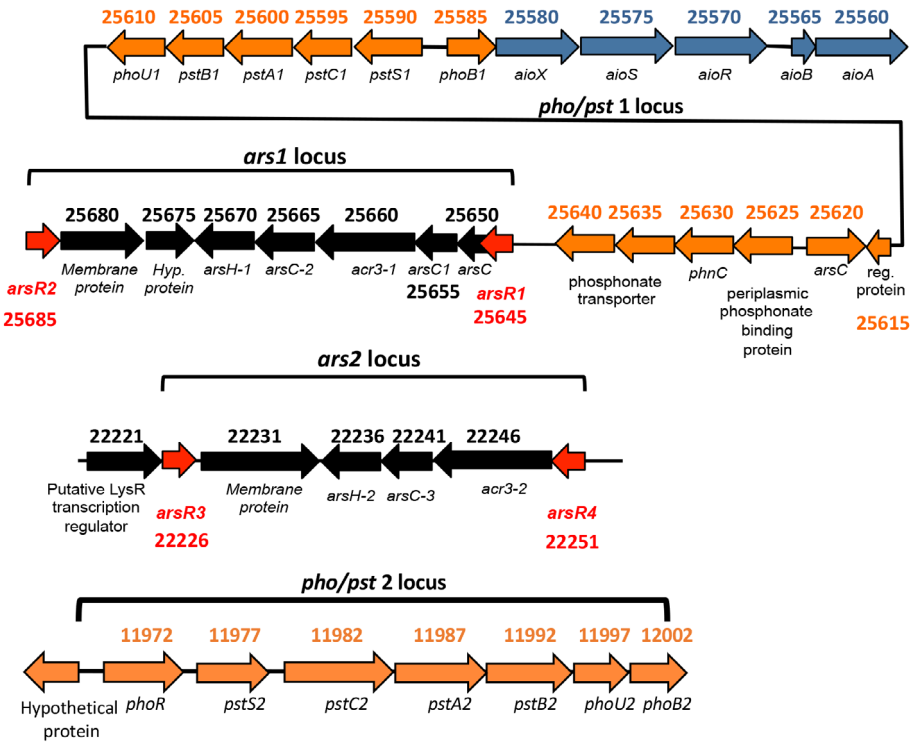

Fig. 1. Genome organization of *aio* (blue), *pst/pho* (orange) and *ars* (black) operons in *A. tumefaciens* 5A. The *arsR* genes encoding As^{III}-sensitive transcriptional repressors are highlighted in red. Gene names are located below arrows and AT5A gene IDs are listed above. Figure adapted from Kang and colleagues (2016).

2006; Liu *et al*., 2012). A periplasmic As^{III}-sensing protein, AioX, senses As^{III} and initiates a signal cascade involving a transmembrane histidine kinase, AioS and its cognate regulatory response partner, AioR. Phosphorylated AioR then initiates transcription of the As^{III} oxidase structural genes (*aioBA*), thereby inducing As^{III} oxidation. More recently, key findings indicate that As^{III} oxidation is sensitive to phosphate levels, to the extent that expression of *aioBA* as well as *aioSR* is controlled by the phosphate stress response (PSR) (Kang *et al*., 2012b; Wang *et al*., 2018). The PSR genes (Pho/Pst) are also regulated via a signal transduction system, in this case involving the histidine sensor kinase PhoR and its cognate regulatory partner PhoB (Hsieh and Wanner, 2010). In *A. tumefaciens* 5A, there are two *pho*/*pst* loci; the *pho*/*pst1* locus is located directly adjacent to the *aio* gene cluster (Fig. 1), whereas the *pho*/*pst2* locus is located elsewhere in the genome (genome sequence not closed, therefore, exact distance is unknown). Recent studies have linked the function and regulatory control of these two systems, where PhoR (*pho*/*pst2* locus, Fig. 1) is the master regulator controlling expression of *aioSRBA*, and thus, As^{III} oxidation (Hao *et al*., 2012; Kang *et al*., 2012b; Wang et al., 2018). These studies have been instrumental in providing a foundational description of the genetic circuitry that controls regulation of As^{III} oxidation in organisms that carry the regulatory genes *aioXSR.*

Despite these advances in describing the regulation of As^{III} oxidation, the global cellular impacts of the Pho/Pst and Aio regulatory systems remain poorly characterized. The cellular functions affected by As^{III} as well as the regulatory effects of both the Pho and Aio systems during As^{III} oxidation remain to be fully explored. To address this, we used a high-throughput RNA sequencing platform to obtain gene expression profiles to define the cellular functions regulated in response to As^{III} exposure, and more specifically, via the two histidine kinases, AioS and PhoR in *A. tumefaciens* 5A.

We document and catalogue transcription changes of 1544 genes in total, encompassing numerous cell functions. This is quite robust in scope and so herein we elected to emphasize specific classes of cellular functions that are well represented with respect to number of genes influenced (i.e. major cellular responses), but that also represent novelty with respect to our understanding of As^{III} oxidation. In particular, we provide some focus on the *aio* and two different *pho*/*pst* loci (Fig. 1), wherein we have previously documented significant and complex regulatory changes (Kang *et al*., 2012b; 2016; Wang *et al*., 2018).

Results

General considerations

All comparisons and contrasts were between uniformly treated cells and thus transcriptional changes can be used to demarcate the PSR, As^{III} effects, and/or the regulatory influences of PhoR or AioS as defined by the

respective mutants, *phoR* and *aioS.* Initial analyses set out to characterize the cellular functions impacted in wild type cells actively growing in 100 μM As(III), while experiencing a PSR condition, which is a prerequisite for induction of As^{III} oxidation (Kang *et al*., 2012b). A complete list of all significant changes in gene expression resulting from As^{III} exposure and/or due to mutations in *phoR* or *aioS* is provided in Supporting Information Table 1. Expression changes are grouped alphabetically by function. Note that depending on perspective, some of these genes could be placed in other functions; for example glyoxylate metabolism is also part of carbon metabolism.

As^{III} exposure has global effects in wild type cells

Comparing gene expression profiles of wild type *A. tumefaciens* 5A cultured with and without As^{III} (100 μM) showed differential regulation of 483 genes; 232 upregulated and 250 downregulated (Table 1 and Supporting Information Table 1). Grouping the genes according to function illustrated a truly global response, involving the perturbation of a wide range of cellular processes (Table 1 and Supporting Information Table 1). Differences in regulation included phenomena that were expected based on prior work (Kashyap *et al*., 2006; Kang *et al*., 2012b; 2015; Wang *et al*., 2018), such as upregulation of *aio* genes (twofold to 87-fold increase), arsenic resistance (threefold to 110-fold) and *pho*/*pst1* locus genes (twofold to 555-fold; see Fig. 1). However, there were several upregulated functional categories that are novel, including carbohydrate metabolism (19 genes, twofold to eightfold), oxidoreductase/electron transport (18 genes, twofold to-147-fold), various transporter activities (22 genes, twofold to sixfold), as well as genes encoding some aspect of copper tolerance (six genes, twofold to 21-fold).

Downregulated processes included 41 genes coding for various aspects of iron metabolism and transport, along with 91 genes annotated as transporters for a very wide variety of solutes (Supporting Information Table 1). In contrast to upregulation of the *pho*/*pst1* locus, genes in the *pho*/*pst2* locus were downregulated (Table 1 and Supporting Information Table 1; Fig. 1) (discussed further below). Overall, it is clear that As^{III} induces a broad response that affects cell metabolism at a variety of levels and in a very large number of functional categories.

PhoR exerts system-wide transcriptional regulation

A visual summary of transcriptional activity in the *phoR* mutant as compared to wild type is provided in Fig. 2A and B, and listed in Table 1. In the comparison between the wild type and Δ*phoR* mutant, nearly 800 genes were differentially regulated in the absence of As^{III} (Table 1 and Fig. 2). Lack of a functional PhoR resulted in reduced expression of 493 genes, illustrating how PhoR-based signalling normally initiates positive regulatory influences under the PSR growth conditions imposed. In addition, loss of PhoR resulted in enhanced expression of 286 genes, showing that many functions are somehow normally repressed in a way that involves PhoR function (Table 1 and Supporting Information Table 1; Fig. 2A and B). Functions most affected include carbohydrate and amino acid metabolisms, iron acquisition, detoxification and stress responses, virulence factors and redox. Transport functions were the most severely disrupted; expression of 147 genes was reduced, most of which by twofold to fourfold, although some were reduced >100-fold (Supporting Information Table 1). The most dramatic example is a phosphonate ABC transporter substrate-binding protein reduced 286-fold (Supporting Information Table S1).

Differential regulation in the Δ*phoR* mutant in response to As^{III} was similarly large (Fig. 2B). Significant changes for a total of 792 genes were noted; 433 genes expressed at lower levels and 358 expressed at higher levels than the wild type (Supporting Information Table 1). Transcription increases were primarily in the twofold to fivefold range, although, there were a few instances where increases were as high as 24-fold (sulfatase gene). Most of the same functional categories were as observed in the $-As^{III}$ Δ*phoR*:WT comparison discussed above; however, in many cases different genes were involved (Supporting Information Table 1). Increased expression ratios for many genes were similar for both $+As^{III}$ and $-As^{III}$ cultures, implying little-to-no As^{III} effect; examples here include genes annotated as being involved in translation, nickel transport, nucleotide metabolism and ATP synthase (Supporting Information Table 1). Significant As^{III}-associated transcription decreases include genes involved in carbohydrate metabolism (twofold to 41-fold decrease), LPS synthesis (twofold to 134-fold decrease), metalloproteins (twofold to 75-fold decrease), transport (twofold to 160-fold decrease) and methyltransferase activity (twofold to 96-fold decrease). A full list of the genes/functions impacted in the Δ*phoR* mutant are provided in Supporting Information Table 1.

AioS exhibits a much smaller regulatory profile

The same experiments and analysis with the Δ*aioS* mutant revealed a smaller regulatory footprint. In the absence of As^{III}, the expression of only 13 genes in six functional categories was altered (Fig. 2C and Table 1), including redox (two genes, twofold to fourfold decrease), phage proteins (two genes, twofold decrease) and transport (three genes, twofold to 3.6-fold). In the presence of As^{III}, a much more extensive regulatory role of AioS was

Table 1. A summary of selected cell functions influenced by arsenite and/or by loss of PhoR or AioS.

			Without arsenic				With arsenic			
	WT (+As) / (−As)		△*phoR* / WT		△*aioS* / WT		△*phoR* / WT		△*aioS* / WT	
Function	Down	Up	Decreased	Increased	Decreased	Increased	Decreased	Increased	Decreased	Increased
Amino acid metabolism	8	2	8	29			12	18	3	
Arsenic resistance		16						7	4	5
Arsenite oxidation		5	1		2		5		4	
Biotin metabolism			4						2	
Carbohydrate metabolism	11	19	32	10			48	13	3	
Cell division	2			4				3	1	
Cobalamin metabolism	2	1		3						
Conjugal transfer								1	7	
Copper tolerance/metabolism	1	6	3	5				2		
Detoxification/stress Response/virulence	6	16	34	5			39	17	3	5
DNA activity	5	6	12	32			15	24	4	1
Fe-S cluster biosynthesis	5			1						
Glycerol/fatty acid metabolism	1	1	19	8			18	13	2	
Iron-chelation (siderophores)	18		10				1		1	
Membrane	13	9	15	8			19	11		
Metal-related function	1	5	8	3			9	4		1
Methyltransferase activity	6	4	6	4			7	6	3	1
Motility/environmental sensing	8	4	3	3			7			
Nitrogen metabolism	7	3	2	5			10	3	2	
Oxidoreductases/electron carry	9	18	48	24	2		36	26	7	
Phage		2	1	1	2			27	23	
Phosphate/phosphonate metabolism	12	17	41	18			51	19	6	10
Sulfur metabolism	3	3	2	4				6	1	
Transcriptional regulation	14	7	10	13			12	36		
Translation	1	17	5	33			6	10	1	
Transport	91	22	147	25	2	1	76	46	21	1
Other	5	6	21	13	1		16	21	3	2
Uncharacterized	21	43	61	35	1	2	46	45	15	6
Total	250	232	493	286	10	3	433	358	116	32

For each function category, the total number of genes with statistically significant altered transcription ratios are shown.

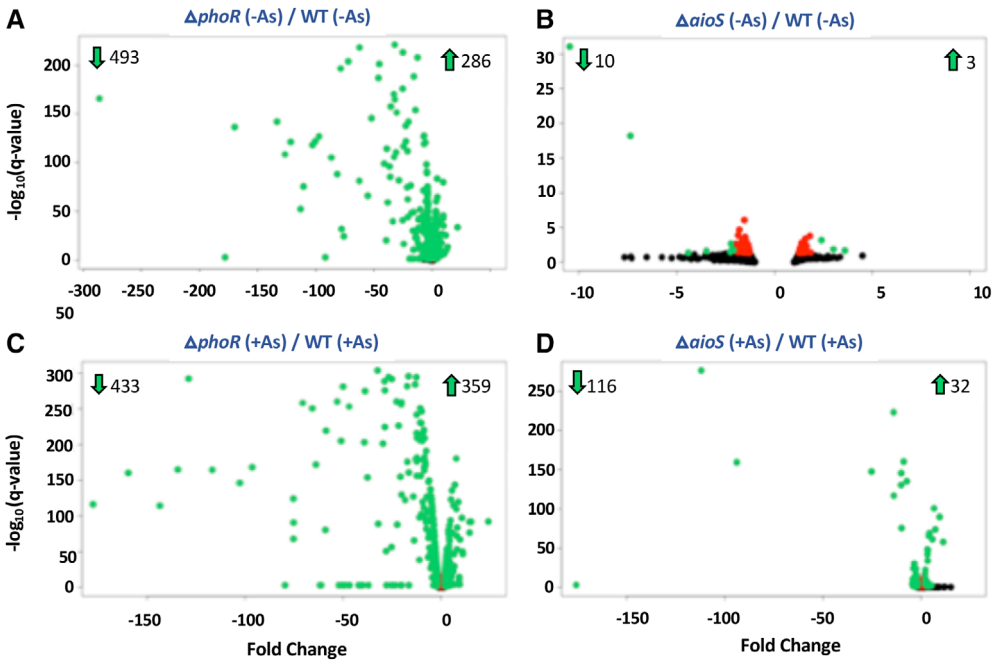

Fig. 2. Volcano plot visual summarization of differential gene expression as influenced by strain genotype and by As^{III} exposure. Red dots indicate a fold change >2, green dots indicate a fold change >2 and a *q* value < 0.05. Note *Y*-axis scale differences.

observed in Δ*aioS* cells: 116 genes were expressed at significantly lower levels than in the wild type strain and 32 genes were expressed at higher levels (Fig. 2D and Table 1). This finding implies that AioS-based regulation normally enhances expression of 116 genes and decreases expression for 32 genes. Numerous cell activities appear to be affected, including conjugal transfer, phage biology and transport activities (Supporting Information Table 1). Briefly summarizing, these findings indicate that AioS plays a much larger regulatory role, directly or indirectly, during As^{III} exposure than previously known. Specific functions influenced by PhoR and AioS will now be examined in more detail, below.

Arsenic resistance and As^{III} oxidation

Expression of the arsenic detoxification genes at the *ars1* and *ars2* loci in the wild type was upregulated in As^{III} exposed cultures (Table 2). This is consistent with our prior work (Kang *et al*., 2012b; 2016) and was expected. Relative to wild type cells, expression of these genes was essentially unaltered in either mutant in the absence of As^{III} (Table 2). In As^{III}-exposed Δ*aioS and* Δ*phoR* mutants, the *ars1* locus was unaffected except for *arsR2*, where expression was reduced approximately threefold in the *aioS* mutant. Expression of an uncharacterized *ars* locus (AT5A_25235, 25240, 25245) was also upregulated in the wild type (Table 2), although, generally at lower levels than observed for genes in the *ars1* and *ars2* loci and similarly reduced in the *aioS* mutant, implying these genes may require AioS for As^{III} induction. Both AioS and PhoR appear necessary for controlling expression of the *ars2* operon (Fig. 1) in a repressing manner (Table 2 and Supporting Information Table 1) and includes the regulatory protein ArsR4, which has its own regulatory footprint (manuscript in preparation).

The different regulatory patterns of the *aio* genes observed for the wild type and mutants offer new insight into the regulation of As^{III} oxidation (Table 2). Several important observations should be noted: (i) in wild type cells, *aioX*, *aioS* and *aioR* were all similarly induced (~twofold to threefold), whereas *aioB* and *aioA* transcript abundance was an order of magnitude greater (Table 2); (ii) *aioX* induction by As^{III} appears uninfluenced by AioS but requires PhoR (consistent with Wang *et al*., 2018); (iii) *aioB, aioA, aioR* and *aioS* require both AioS and PhoR (Table 2); (iv) *aioB* and *aioA* are upregulated to different extents in the wild type cell (~threefold difference), illustrating that transcription of these genes is somehow uncoupled, although this difference largely disappears in either mutant (Supporting Information Table 1); and (v) in the absence of As^{III}, *aioB* expression, but not *aioA*, was significantly reduced in both mutants (about the same level), indicating that both AioS and PhoR are somehow necessary for *aioB* expression in the absence of As^{III} (Table 2).

Phosphate stress response

Strain 5A contains two loci with several genes annotated as encoding elements of the PSR (Fig. 1), and in addition

Table 2. Influence of arsenite and △phoR and △aioS mutations on the expression of genes involved with arsenic resistance and arsenite oxidation.

				Mutant Versus Wild type			
				No AsIII		With AsIII	
Uniprot identifier		Annotation	Wild type (+As/−As)	△*phoR*	△*aioS*	△*phoR*	△*aioS*
ars 2 locus							
* AT5A_22226	*arsR3*	ArsR family transcriptional regulator					
AT5A_22231		Major facilitator transporter	4.6			7.6	5.9
AT5A_22236	*arsH-2*	Monomethylarsenite oxidase	15.4			6.9	6.7
* AT5A_22241	*arsC-3*	Arsenate reductase	16.6			7.6	7.3
AT5A_22246	*acr3-2*	Arsenite efflux pump protein	15.3			8.6	9.5
AT5A_22251	*arsR4*	ArsR family transcriptional regulator	13.7			10.7	11.3
Uncharacterized *ars* locus							
* AT5A_25235	*arsC*	Arsenate reductase	3.9				−3.4
AT5A_25,240	*arsC*	Arsenate reductase	5.5				−3.8
AT5A_25,245	*arsR*	ArsR family transcriptional regulator	3.2				−2.8
ars 1 locus							
AT5A_25620	*arsC*	ArsR family transcriptional regulator	43.8				
AT5A_25645	*arsR1*	ArsR family transcriptional regulator	45.1				
AT5A_25650	*arsC*	Arsenate reductase	65.1				
* AT5A_25655	*arsC1*	Arsenate reductase	109.6				
AT5A_25660	*acr3-1*	Arsenite efflux pump protein	96.2				
AT5A_25665	*arsC-2*	Arsenate reductase	88.1				
AT5A_25670	*arsH*	Monomethylarsenite oxidase	69.2				
AT5A_25685	*arsR2*	ArsR family transcriptional regulator	8.0				−2.9
Arsenite Oxidation							
AT5A_25550	*aioD*	Molybdenum cofactor synthesis domain-containing protein	15.7			−10.0	−25.1
* AT5A_25555	*aioC*	Cytochrome C class I	147.2			−25.3	−175.5
AT5A_25560	*aioA*	Arsenite oxidase large subunit	87.1			−22.5	−111.9
AT5A_25565	*aioB*	Arsenite oxidase small subunit	26.9	−5.9	−7.4	−32.0	−93.7
AT5A_25570	*aioR*	Cognate regulator paired with AioS; controls *aioBA* expression	2.0			−3.2	−2.6
* AT5A_25575	*aioS*	AioS sensor kinase that controls *aioBA* expression	2.3		NA	−2.7	NA
AT5A_25580	*aioX*	Periplasmic arsenite-sensing protein; involved in *aioBA* regulation	3.3			−3.7	

Genes are listed according to their Uniprot identifier in increasing order. Genes that share physical proximity and orientation such that they may be in the same operon are marked with an * and highlighted in light gray blocks. NA, not applicable. Lack of fold change indicates expression changes did not meet the base criteria of (±) twofold change and p value < 0.05.

another locus containing a large cluster of genes encoding phosphonate acquisition and metabolism. All genes in the *pho*/*pst1* locus were upregulated by As^{III} in the wild type (~20- to >550-fold, Table 3), whereas the phosphonate locus was not influenced and the *pho*/*pst2* locus was uniformly downregulated threefold to fourfold by As^{III} (Table 3).

Based on expression changes in the Δ*phoR* mutant, the phosphonate component of the PSR appears regulated through only PhoR (as expected), whereas both signal transduction systems (PhoR and AioS) are involved in regulating the two different *pho*/*pst* loci, although with opposing effects (Table 3). As^{III} effects on transcription in the Δ*phoR* strain were variable; for example genes associated with metabolism of polyphosphate (*ppk*, *ppx*) and phosphonate (*phnN*, *phnM*) were not influenced, whereas expression of the *phnE1,E2*, *phnCLKJ* and *phnIHG* phosphonate operons and the *pho*/*pst2* locus were significantly reduced in the Δ*phoR* mutant as compared to wild type (Table 3). Even though these genes appeared unaffected by As^{III} in the wild type, As^{III} did nevertheless influence their expression in the Δ*phoR* mutant. In the absence of As^{III}, loss of PhoR had variable effects (downregulated 0- to 25-fold), suggesting the existence of PhoR-PhoB associated promoters in the *pho*/*pst1* locus region involving phosphonate metabolism.

While less robust, PSR regulatory patterns involving AioS were evident. Upregulation of *pho*/*pst2* locus genes in the $+As^{III}$ Δ*aioS* mutant near perfectly matched the downregulation in the $+As^{III}$ wild-type strain (Table 3), inferring the role of AioS in constraining the expression of the *pho*/*pst2* in As^{III} exposed wild type cells (in parallel with *aio* gene induction, Table 2). During As^{III} exposure, expression of the *pho*/*pst1* locus genes (directly adjacent to the *aio* operon, Fig. 1) in both mutants was lower than the wild type, with Δ*phoR* having a larger effect on expression than

Table 3. Influence of arsenite and/or the △phoR and △aioS mutations on the expression of genes involved with phosphorus acquisition and metabolism.

	Uniprot identifier		Annotation	Wild type (+As/–As)	Mutant versus Wild type			
					No AsIII		With AsIII	
					△*phoR*	△*aioS*	△*phoR*	△*aioS*
	Phosphonate locus							
*	AT5A_05580	*ppk*	Polyphosphate kinase		–8.3		–10.9	
	AT5A_05585	*ppx*	Exopolyphosphatase		–2.3		–2.7	
	AT5A_10767	*phnN*	Ribose 1,5-bisphosphate phosphokinase		–7.3		–8.8	
*	AT5A_10772	*phnM*	Phosphonate metabolism protein		–7.1		–8.9	
	AT5A_10777		UP - putative phosphonate metabolism protein		–7.0		–7.0	
	AT5A_10782	*phnE1*	Phosphonate ABC transporter, permease protein		–91.7		–32.4	2.0
	AT5A_10787	*phnE2*	Phosphonate ABC transporter, inner membrane subunit	–2.2	–178.0		–52.1	2.2
	AT5A_10792		Phosphonate ABC transporter substrate-binding protein		–286.0		–128.8	
*	AT5A_10797	*phnC*	Phosphonates import ATP-binding protein		–169.7		–65.6	2.2
	AT5A_10807	*phnL*	Phosphonate ABC transporter nucleotide-binding protein/ATPase		–30.6		–50.5	
	AT5A_10812	*phnK*	Phosphonate C-P lyase system protein		–22.6		–37.0	
	AT5A_10817	*phnJ*	Alpha-D-ribose 1-methylphosphonate 5-phosphate C-P lyase		–31.1		–46.7	
	AT5A_10822		UP - predicted transmembrane protein 98		–12.3		–28.0	
	AT5A_10827	*phnI*	Phosphonate metabolism protein		–7.5		–13.3	
*	AT5A_10832	*phnH*	Carbon-phosphorus lyase complex subunit		–41.3		–61.2	
	AT5A_10837	*phnG*	Phosphonate metabolism protein		–46.2		–48.9	
	***pho/pst 2* locus**							
	AT5A_11972	*phoR*	Two component sensor histidine kinase		NA		NA	
	AT5A_11977	*pstS2*	Phosphate ABC transporter substrate-binding protein	–3.3	–133.4		–39.1	3.5
	AT5A_11982	*pstC2*	Phosphate transport system permease protein	–3.7	–78.7		–21.7	4.4
*	AT5A_11987	*pstA2*	Phosphate transport system permease protein	–3.5	–72.2		–20.2	4.1
	AT5A_11992	*pstB2*	ABC phosphate transporter, ATP-binding protein	–3.3	–32.8		–12.4	3.6
	AT5A_11997	*phoU2*	Phosphate-specific transport system accessory protein	–3.2	–21.5		–8.2	3.3
	AT5A_12002	*phoB2*	Phosphate regulon transcriptional regulatory protein	–3.5	–21.2		–7.5	3.4
	***pho/pst 1* locus**							
*	AT5A_25585	*phoB1*	Phosphate regulon transcriptional regulatory protein PhoB	46.7			–16.5	
	AT5A_25590	*pstS1*	Phosphate binding protein	554.8	–3.9		–177.5	–13.9
	AT5A_25595	*pstC1*	Phosphate transport system permease protein	160.7			–58.7	–10.0
*	AT5A_25600	*pstA1*	Phosphate transport system permease protein	172.4	–2.0		–49.9	–8.8
	AT5A_25605	*pstB*	ABC phosphate transporter, ATP-binding protein	183.8			–46.8	–10.1
	AT5A_25610	*phoU1*	Phosphate-specific transport system accessory protein	124.4			–37.6	–9.8
	AT5A_25615		Phosphate regulon transcriptional regulatory protein	119.8			–16.6	–7.2
*	AT5A_25625		Phosphonate ABC transporter, periplasmic binding protein	23.3	–24.5		–116.7	
	AT5A_25630	*phnC*	Phosphonates import ATP-binding protein	23.2	–11.7		–50.9	
	AT5A_25635		Phosphonate ABC transporter, inner membrane subunit	21.0	–5.9		–29.6	
	Other							
*	AT5A_12927		Phosphate transporter				–2.2	
	AT5A_12942		Sucrose-phosphate phosphatase (Fragment)		2.4		2.4	
	AT5A_16076		Phosphate ABC transporter ATP-binding protein	–2.0	–2.3			
*	AT5A_16561		Phosphate permease		13.3		6.2	
	AT5A_16566		Putative pit accessory protein		9.6		5.6	
*	AT5A_18626	*ppa*	Inorganic pyrophosphatase (Pyrophosphate phospho-hydrolase)		2.0			
	AT5A_24150	*PhnD*	UP - phosphonate transport system, periplasmic component				2.8	

Genes are listed according to their Uniprot identifier in increasing order. Genes that share physical proximity and orientation such that they may be in the same operon or are clustered so to enhance the possibility of coordinated transcription are marked with an * and highlighted in light gray blocks. Gene elements of the *pho1*/*pst1* and *pho2*/*pst2* loci (depicted in Fig. 1) are as designated. UP, uncharacterized protein. NA, not applicable. Lack of fold change indicates expression changes did not meet the base criteria of (±) twofold change and p value < 0.05.

the Δ*aioS* mutation. Thus, AioS and PhoR appear necessary for optimal expression of most of the *pho*/*pst1* locus during As^{III} exposure, with the exception of *phoB1*, which is transcribed divergently from the rest of the operon (Fig. 1) and not affected by the Δ*aioS* mutation.

Iron acquisition

In the wild type cells, expression of a surprisingly large contingent of genes encoding functions associated with iron acquisition/metabolism were affected by As^{III} (twofold to

56-fold, Table 4). Expression of 41 genes in 14 different apparent operons were altered, with all but one gene downregulated and with most annotations implying some type of iron transport or regulation activity. This was not a random coincidental change in transcription, but rather a well-organized cell response. For the most part, expression changes within apparent operons were uniform for all genes involved, although, there were instances where some genes were expressed at much higher levels (e.g. AT5A_23525, AT5A_23530, AT5A_23535; Table 4), perhaps explained by either differences in mRNA half-life or additional promoters within the gene clusters (putative operons). Most of these transcriptional changes are governed in some fashion by PhoR (Table 4), whereas AioS appears to be of little influence on this category of function. The *phoR* mutation resulted in various patterns of transcriptional changes; some that were mutually exclusive with respect to presence or absence of As^{III}, and others where the addition of As^{III} resulted in attenuation of the downregulation effect seen in the wild type cell (e.g. AT5A_07245, AT5A_07250) or exerted a repressive effect where there was none in the wild type (e.g. AT5A_15751, AT5A_15756, AT5A_15761, AT5A_15766; Table 4).

Phage biology and conjugal transfer

Genes associated with phage biology were affected in both mutants, primarily in response to As^{III} exposure (Table 5). This involved perturbation of four distinct operons encoding 37 proteins (Table 5). The effects were largely antagonistic between mutants in the presence of As^{III}; i.e., all genes exhibiting increased expression in the *phoR* mutant were decreased in the *aioS* mutant. Another surprise was to learn that AioS impacts genes involved in conjugal transfer (Table 5). This was not evident in As^{III}-treated wild type cells nor in the Δ*phoR* mutant, but as with most transcriptional perturbations noted in this study, the effects included entire operons, and thus, not likely to be nonrandom or spurious.

Carbohydrate metabolism

As^{III} perturbations of genes encoding aspects of carbohydrate metabolism were very apparent (Table 1). In the wild-type, 19 genes were upregulated, including phosphoenolpyruvate carboxykinase, acetate kinase, glucose dehydrogenase, glycogen synthase and in particular glycoside metabolism (Supporting Information Table 1). Transcripts encoding eight proteins responsible for sugar conversions, galactose metabolism and glyoxylate/dicarboxylate were all downregulated. Additionally, a considerable number of sugar transporters were downregulated in the wild-type (27 genes, twofold to 3.5-fold). AioS appears to have little regulatory influences over this category of cell function. By contrast, loss of PhoR resulted in reduced expression of 32 genes in the absence of As^{III} and 48 genes in As^{III} treated cells (up to 41-fold; Supporting Information Table 1). For the Δ*phoR* mutant and in the absence of As^{III}, major transcriptional reductions occurred with genes encoding glycoside metabolism. The addition of As^{III} resulted in further decreased expression for many of these same genes, as well as decreased expression of genes encoding aspects of exopolysaccharide synthesis (Supporting Information Table 1).

Amino acid metabolism

Amino acid metabolism is another major aspect of cellular metabolism that was influenced by As^{III} (Table 1). In the wild type, alanine racemase and ornithine decarboxylase were upregulated (2.5- to 2.8-fold respectively; Supporting Information Table 1), whereas genes encoding reactions involved in the synthesis of glutamate, glutamine, lysine, cysteine, methionine and phenylalanine were downregulated (twofold to sixfold). As noted above for carbohydrate metabolism, AioS appears to exert little influence on amino acid metabolism, whereas again PhoR plays an important regulatory role, although varying as a function of As^{III}. In the absence of As^{III}, transcription of 37 genes in this category were altered in the Δ*phoR* mutant. Of these, 29 genes were increased, with glycine (four genes) and histidine (eight genes) metabolism particularly influenced. When As^{III} was included in the medium, 30 amino acid-related genes were affected relative to wild type. But of these, seven were not changed substantially from the *phoR* $-As^{III}$ condition, and thus we conclude that their expression was dependent on PhoR, and independent from As^{III} (Supporting Information Table 1).

Other functions influenced

Substantive changes in transcript abundance for a variety of other functions was also observed and are important to discuss in the context of identifying novel regulatory influences by As^{III}, PhoR, AioS or combinations thereof. The wild type arsenic response included increased transcription of copper tolerance/metabolism genes, with PhoR apparently playing an important role in this regard (Supporting Information Table 1). Likewise, PhoR also is involved in controlling functions associated with detoxification and stress response (Supporting Information Table 1). Fe-S cluster biosynthesis is downregulated in the wild type, but this response appears to be largely controlled by some other regulatory pathway because PhoR and AioS do not appear to be involved. Some aspects of chemotaxis were repressed, whereas others

Table 4. Influence of arsenite and △phoR and △aioS mutations on the expression of genes involved with iron acquisition and metabolism.

				Mutant versus Wild type			
				No AsIII		With AsIII	
	Uniprot Identifier		Annotation	Wild type (+As/–As)	△*phoR*	△*aioS*	△*phoR*	△*aioS*
*	AT5A_00040		Periplasmic chelated iron-binding protein					–2.5
	AT5A_00050		Iron ABC transporter ATP-binding protein	2.4			3.0	–3.7
	AT5A_01130	*fecR*	Protein fecR				–2.0	
	AT5A_01140		Iron ABC transporter nucleotide binding/ATPase protein	–3.4				
	AT5A_01145		Iron ABC transporter membrane spanning protein	–3.5				
*	AT5A_01150		Iron ABC transporter substrate binding protein	–4.0				
	AT5A_01155		Iron ABC transporter substrate binding protein	–5.1				
	AT5A_01170		Iron ABC transporter nucleotide binding/ATPase protein	–2.8	–4.8			
	AT5A_01175		Iron ABC transporter membrane spanning protein	–3.5	–8.1			
	AT5A_01180		Iron ABC transporter substrate binding protein		–8.8		–2.2	
	AT5A_02730	*hemH*	Ferrochelatase (Heme synthase) (Protoheme ferro-lyase)				–2.1	
	AT5A_05970		Iron III ABC transporter, periplasmic iron-binding protein					3.3
*	AT5A_05975		Fe III dicitrate ABC transporter, permease		–3.5			
	AT5A_05990		Ferritin		–2.2			
*	AT5A_07245		Ferric transport system permease protein		–25.2		–10.5	
	AT5A_07250		Iron-binding periplasmic protein		–86.6		–38.8	
	AT5A_07915		Iron III-binding periplasmic protein		–6.2		–8.6	
	AT5A_08610		TonB-dependent heme receptor A	–22.2				
	AT5A_09670		Iron-chelator utilization protein	–12.2				
	AT5A_09690	*hmuV*	Hemin import ATP-binding protein HmuV	–12.0				
*	AT5A_09695		Hemin ABC transporter transmembrane protein	–18.7				
	AT5A_09700		Hemin ABC transporter substrate-binding protein	–24.2				
	AT5A_09710	*huvX*	Heme utilization protein	–21.6				
	AT5A_10045		Catechol 1,2-dioxygenase		–2.3			
	AT5A_10110		Iron ABC transporter substrate-binding protein				2.1	
	AT5A_10742		TonB protein	–25.0				
	AT5A_11337		Iron-regulated protein	–8.5				
*	AT5A_11917		Iron ABC transporter nucleotide-binding protein/ATPase	–5.7				
	AT5A_11922		Iron ABC transporter substrate-binding protein	–5.7			2.2	
	AT5A_15751		Iron ABC transporter, membrane spanning protein				–2.6	
*	AT5A_15756		Iron ABC transporter, membrane spanning protein				–2.6	
	AT5A_15761		Iron ABC transporter nucleotide-binding protein/ATPase				–2.6	
	AT5A_15766		Iron ABC transporter substrate binding protein				–2.7	
	AT5A_16281		Iron ABC transporter substrate binding protein	–2.2				
	AT5A_16421		Ferrichrome ABC transporter	–3.2				
*	AT5A_16431		Ferrichrome transport system permease	–2.2				
	AT5A_16436		Ferrichrome ABC transporter	–3.0				
*	AT5A_19861		Fec I like protein	–12.0				
	AT5A_19866	*fecR*	FecR protein	–5.6				
*	AT5A_20066		Iron ABC transporter transmembrane protein		–2.7			
	AT5A_20071		Iron ABC transporter substrate-binding protein	–2.1	–5.0		–2.1	
	AT5A_22561		Hydroxamate-type ferrisiderophore receptor		–2.6			
*	AT5A_22566		Ferrichrome ABC transporter substrate binding protein	–5.7				
	AT5A_22571		Iron-hydroxamate transporter permease subunit	–4.0				
	AT5A_22576		Ferrichrome ABC transporter nucleotide-binding protein/ATPase	–5.9				
	AT5A_23490		TonB-dependent siderophore receptor	–21.0				
	AT5A_23505		Iron ABC transporter, ATP binding protein	–7.5				
	AT5A_23510		Iron ABC transporter permease	–3.5				
	AT5A_23515		Iron ABC transporter permease	–4.6				
*	AT5A_23520		Iron ABC transporter periplasmic iron-binding protein	–6.4				
	AT5A_23525		Siderophore-interacting protein	–24.4				
	AT5A_23530		UP - Periplasmic-binding (Phosphopantetheine attachment site)	–20.2				
	AT5A_23535		Agrobactine synthetase subunit F	–17.3	–10.3			
*	AT5A_23540		Agrobactine synthetase subunit F	–11.0	–6.4			
	AT5A_23545		Nonribosomal peptide synthetase module	–19.3				

(Continues)

Table 4. Continued

	Uniprot Identifier		Annotation	Wild type (+As/–As)	Mutant versus Wild type			
					No AsIII		With AsIII	
					△*phoR*	△*aioS*	△*phoR*	△*aioS*
	AT5A_23550		Isochorismate synthase		–18.4			
	AT5A_23555	*entE*	Enterobactin synthase subunit E	–53.5	–19.5			
*	AT5A_23560		2,3-dihydro-2,3-dihydroxybenzoate synthetase	–56.0	–19.2			
	AT5A_23565		2,3-dihydroxybenzoate-2,3-dehydrogenase	–39.6	–16.3			
	AT5A_23570		Phosphopantetheinyl transferase	–15.3	–12.0			
	AT5A_23705		Iron ABC transporter periplasmic solute-binding protein		–2.0			
*	AT5A_23715		Iron ABC transporter periplasmic solute-binding protein		–2.0			
	AT5A_23725		Iron ABC transporter permease					–2.2

Genes are listed according to their Uniprot identifier in increasing order. Genes that share physical proximity and orientation such that they may be in the same operon or are clustered so to enhance the possibility of coordinated transcription are marked with an * and highlighted in light gray blocks. UP, uncharacterized protein. Lack of fold change indicates expression changes did not meet the base criteria of (±) twofold change and p value < 0.05.

were activated and again PhoR was often involved. Other functions wherein PhoR exerts some type of regulatory control include synthesis of biotin and cobalamin (both in the absence of $-As^{III}$), LPS synthesis ($\pm As^{III}$), Type VI secretion system ($\pm As^{III}$), nucleotide metabolism, glycerol/fatty acid metabolism ($\pm As^{III}$), oxidoreductases and sulfur metabolism.

Motif searches

Pho boxes are well recognized as PhoB binding sites and are characterized as an important regulatory component of the PSR (Wanner, 1993; 1996). However, there is little equivalent information concerning AioXSR-based transcriptional controls, and therefore we conducted motif searches focused on Δ*aioS*-perturbed genes to initiate this type of analysis. An important assumption going into this analysis was that transcriptional control of all *aioS*-influenced genes would also involve AioR, the cognate regulatory protein for AioS. Targeted motif searches included binding sites for AioR (Corsini *et al*., 2017; Shi *et al*., 2018) and σ^{54}, which is known to be involved in transcriptional regulation of arsenite oxidase in 5A and *Herminiimonas arsenicoxydans* (Koechler *et al*., 2010; Kang *et al*., 2012a). Searches were conducted within the 300 nucleotide region upstream of the translational start site for each gene.

Of the 148 genes significantly influenced by the Δ*aioS* mutation (with or without As^{III}), potential σ^{54} binding sites were found for 100, the majority (83 genes) of which were positively influenced by AioS (Supporting Information Table 2). Multiple putative σ^{54} binding sites were found for 45 genes (up to six sites per gene), but there was no apparent relationship between σ^{54} binding site abundance and ±change in expression as a function of As^{III} exposure in the Δ*aioS* mutant or wild type strains (data not shown). Distribution within the upstream 300 nucleotide region varied significantly (Fig. 3), with the vast majority residing further upstream from the translational start than normally documented (Cannon *et al*., 1993). Additionally, there was no correlation between σ^{54} binding site motif position and fold change in expression, nor between gene expression levels/patterns as a function of sequence deviations from the search motif (Supporting Information Table 2).

The predicted and experimentally demonstrated degenerate AioR binding site motif (Li *et al*., 2013; Shi *et al*., 2017) and that predicted by Corsini and colleagues (2017) were used to search for potential AioR binding sites (see Supporting Information Table 2). Of the 148 genes influenced in the Δ*aioS* mutant, only slightly over half (78 genes) were associated with one or the other putative AioR-type binding sites (Supporting Information Table 2). The Corsini and colleagues (2017) motif was associated with only 18 of these genes, whereas the motif described by Shi and colleagues (2017) was found associated with 67 genes; seven genes were found to be associated with both motifs. As would be predicted, the degenerate sequence of Shi and colleagues (2017), allowed for greater flexibility and thus it was identified more frequently. We did not observe any relationship between As^{III}-related gene expression and occurrence or abundance of either type of AioR binding site (Supporting Information Table 2).

Discussion

This study summarizes an RNASeq-based in-depth examination of the global impacts of As^{III} exposure on *A. tumefaciens* 5A, a model organism for understanding how and why microbes react to arsenic. In particular, this organism is used to study the genetics and regulation of

Table 5. Influence of arsenite and △phoR and △aioS mutations on the expression of genes encoding phage structural and functional elements, and for conjugal transfer.

				Wild type (+As/−As)	Mutant versus Wild type			
					No AsIII		With AsIII	
	Uniprot Identifier		Annotation		△*phoR*	△*aioS*	△*phoR*	△*aioS*
	Phage related genes							
	AT5A_03465		UP (Fragment) - envelope glycoprotein,				2.5	
	AT5A_04655		Large terminase phage packaging protein	3.0	4.1		2.3	
*	AT5A_04680		Uncharacterized protein					−3.0
	AT5A_04690		Phage phi-C31 major capsid gp36-like protein					−2.5
	AT5A_04695[a]		UP - Head-Tail connector protein					−3.3
	AT5A_04715		TP901-1 family phage major tail protein					−2.9
*	AT5A_04735[a]		UP - Prophage functions					−2.7
	AT5A_04740[a]		UP - Gene transfer agent					−2.6
	AT5A_04750[a]		UP - Phage tail protein					−2.2
	AT5A_08985		UP - Phage_tail_X	2.1				
	AT5A_09015		UP - Phage tail sheath protein				2.2	
	AT5A_09045		Phage-related baseplate assembly protein				2.0	−2.4
	AT5A_09050		GPW/gp25				2.3	−2.7
	AT5A_09060		UP - Type VI secretion system, phage-baseplate injector				2.6	
	AT5A_09065		UP				2.1	
*	AT5A_09075		UP - Predicted phage recombinase			−2.3	3.0	−2.2
	AT5A_09080		Phage terminase GpA				3.3	−2.2
	AT5A_09085		Peptidase U35, phage prohead HK97				2.3	−2.1
	AT5A_09090		Lambda family phage portal protein				2.6	
	AT5A_09095		UP				2.5	−2.1
	AT5A_09100		Phage terminase GpA				2.7	−2.4
	AT5A_09105[a]		UP - Phage DNA packaging protein				2.5	−3.9
	AT5A_09110		UP - Putative addiction module antidote protein			−2.1	3.4	−2.8
	AT5A_09170		UP				2.0	−2.9
	AT5A_14682		UP - Protein of unknown function (DUF3168)				2.2	
	AT5A_14687		UP - Bacteriophage putative tail component				2.5	−2.2
*	AT5A_14692		Phage head-tail adaptor				3.3	
	AT5A_14697		UP				2.7	−2.5
	AT5A_14702		UP - Head-Tail connector protein				3.9	−2.0
	AT5A_14707		UP, histidine kinase				3.4	
	AT5A_14712		UP				3.0	
	AT5A_14717		Phage major capsid protein, HK97 family				3.5	−2.1
*	AT5A_14722		Peptidase S49				2.9	−2.3
	AT5A_14727		Phage portal protein, HK97 family				2.9	
	AT5A_14732		Terminase large subunit				2.8	
	AT5A_14737		Terminase small subunit				2.2	−2.7
	AT5A_14872		UP - DUF669 (in various phage protein families)		−2.2		2.6	
	Conjugal transfer							
	AT5A_24520		Conjugal transfer protein Dtr system					−2.1
*	AT5A_24525	*traC*	Conjugal transfer protein TraC					−2.6
	AT5A_24540	*traB*	Conjugal transfer protein TraB					−2.1
	AT5A_24785		Uncharacterized protein - VirB5-like protein					−2.9
*	AT5A_24795	*trbE*	Conjugal transfer protein TrbE					−2.6
	AT5A_24800	*trbD*	Conjugal transfer protein TrbD					−3.2
	AT5A_24810	*trbB*	Conjugal transfer protein TrbB					−3.0

Genes are listed according to their Uniprot identifier in increasing order. Genes that share physical proximity and orientation such that they may be in the same operon or are clustered so to enhance the possibility of coordinated transcription are marked with an * and highlighted in light gray blocks. UP, uncharacterized protein. Lack of fold change indicates expression changes did not meet the base criteria of (±) twofold change and p value < 0.05.

a. TPM average for one treatment group < 1.

As^{III} oxidation, and thus, a focal point of this study was to examine As^{III} effects on gene expression while the cells are engaged in As^{III} oxidation. To facilitate this, the PSR must be induced because expression of *aioSR* and ultimately *aioBA* is controlled by the PSR (Kang *et al*., 2012b; Wang *et al*., 2018). Therefore, the influence of As^{III} on global expression patterns occurs within a background of the PSR. Nevertheless and as expected, the results also captured responses well documented as induced by As^{III}, but not requiring the PSR (e.g. *ars* genes).

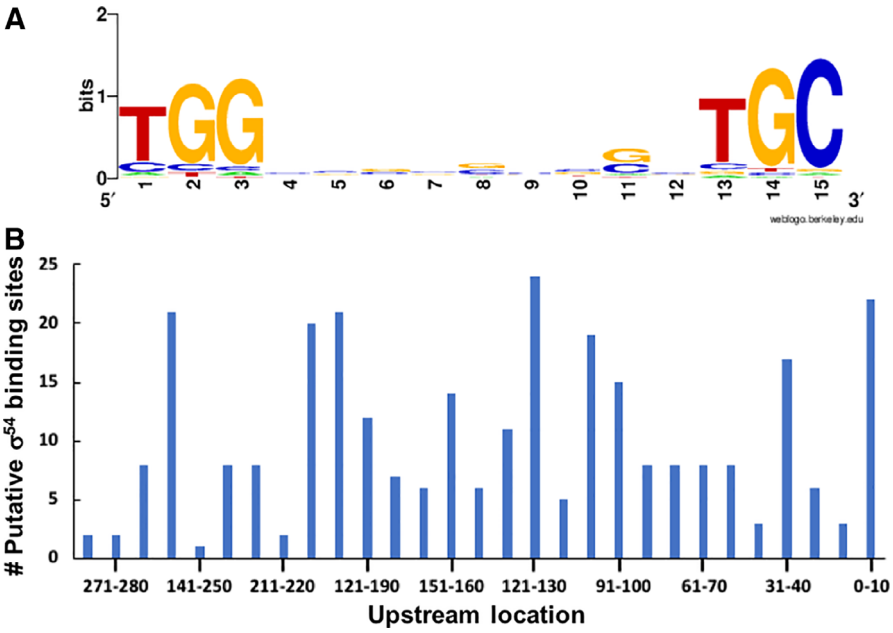

Fig. 3. Identification and distribution of putative σ^{54} binding sites upstream of genes transcriptionally altered in the △*aioS* mutant.
A. Consensus motif sequence for putative binding sites in △*aioS* mutant.
B. Frequency distribution of the s^{54} binding site motifs identified (exact and variants) in 10 nt increments within the upstream 300 bp region for 103 genes controlled (directly or indirectly) by AioS and found to be associated with this motif.

While we provide a comprehensive and function-organized listing of all genes affected, we elected to focus some of our description and discussions on genes/functions previously identified so as to further expand on these important elements of As^{III} responses and As^{III} oxidation. In particular, the genome loci illustrated in Fig. 1 was of interest because past efforts (Kang *et al*., 2012a,b; 2016) have shown this to be a relative 'hot spot' with regards to regulating As^{III} oxidation and arsenic resistance, and how their transcription is integrated with the PSR. As well, we sought to highlight novelty in regards to the current understanding of bacterial responses to As^{III}.

Previous microarray-based As^{III} exposure studies were conducted with *Herminiimonas arsenicoxydans* (Cleiss-Arnold *et al*., 2010) and *Rhizobium* NT-26 (Andres *et al*., 2013). The PSR has yet to be characterized in either organism, but we note that PSR culture conditions used in the current study were very similar to those described for the 'Late Phase' expression patterns of *H. arsenicoxydans* (Cleiss-Arnold *et al*., 2010). A PSR scenario is less clear for *Rhizobium* NT-26 (Andres *et al*., 2013) because of the relatively high starting Pi concentration in the media used (1.25 mM), although this is similar to that used for *A. tumefaciens* strain GW4 (Wang *et al*., 2015; 2018) and thus potentially may have translated to a PSR condition in the stationary phase cells used by Andres and colleagues (2013). To clarify this situation, the PSR needs to be characterized in these organisms so as to determine if there are substantive variations among these bacteria.

Regarding strain 5A wildtype cell responses, upregulation of several specific genes was expected in the presence of As^{III} (e.g. *ars*, *pho/pst1*, *aio*) and is consistent with our prior work (Kang *et al*., 2012b; 2016), illustrating consistency and reproducibility between studies, and accordingly served as internal controls to validate the study in general because the data was acquired from the same batches of mRNA. In terms of general functions, several As^{III}-influenced responses (Table 1) were also observed in the above cited microarray studies (Cleiss-Arnold *et al*., 2010; Andres *et al*., 2013). Examples include stress responses, numerous transport activities, amino acid and nucleic acid metabolisms, etc. (Supporting Information Table 1). However, there were several As^{III}-influenced functions in strain 5A that were not found in reviewing these studies and may stem from the deeper probing capacity of RNASeq relative to the lower sensitivity of microarrays. One prominent example concerns iron. Genes encoding functions associated with different aspects of iron homeostasis were uniformly downregulated (41 genes reduced twofold to 56-fold). This reflected 10 separate putative operons and thus implies a well-organized cellular response (Table 4), with iron transport operons a major target of suppression. Iron reacts with H_2O_2 in the Fenton reaction to generate the $HO^{\cdot}$ radical (see review by Imlay, 2013) and so we speculate that constraining iron uptake might be viewed as one form of oxidative stress response in cells already undergoing oxidative stress brought on by As^{III} exposure. Oxidative stress is a known cellular reaction to As^{III} exposure (Parvatiyar *et al*., 2005) and indeed we observed significant increases in *katG* (catalase-peroxidase), three separate *ahpD* (alkyl hydroperoxide reductases) and two glutathione S-transferase genes linked to PhoR (Supporting Information Table 1). Similar oxidative stress

responses were also reported for *H. arsenicoxydans* and *Rhizobium* NT-26 (Cleiss-Arnold *et al*., 2010; Andres *et al*., 2013). PhoR has a role in controlling these iron genes, although it is apparently linked to substantial upregulation, not downregulation as observed in the wild type cell. As with many other functions, its opposite influence relative to wild-type invokes the role of some other repressive-type regulator that is normally activated by PhoR.

Other novel wildtype strain responses involved differential regulation of the two different *pho*/*pst* loci (Table 3). The *pho*/*pst1* locus genes are highly upregulated in the $+As^{III}$ cells, whereas the *pho*/*pst2* locus is primarily downregulated. Comparing the *phoR* mutant to the wildtype strain in $-As^{III}$ cells illustrates the *pho*/*pst2* locus genes are significantly affected, whereas the *pho*/*pst1* locus is not. By contrast, the *pho*/*pst1* locus genes are highly upregulated by As^{III}, and PhoR nevertheless exerts regulatory influence (Table 4) (Wang *et al*., 2018). In comparing *pho*/*pst2* gene expression changes in the wildtype and *aio*S mutant, it appears that the As^{III}-based repression of the *pst*/*pho2* genes in the wild type strain is associated with AioS-based signalling activity. AioS is also essential for upregulating the As^{III} oxidase genes (*aioBA*) required for synthesizing the phosphate analog, As^{V}, that we hypothesized partially spares Pi in some cellular features (Wang *et al*., 2015; 2018). This differential response and control circuitry of the *pho*/*pst* loci provides new insight as to their role in this bacterium. We consider the *pho*/*pst2* locus to be the primary PSR operon frequently documented as being the foundation of the PSR in various Gram negative bacteria (Wanner and Chang, 1987; Wanner, 1996; Hsieh and Wanner, 2010), however, its apparent AioS-linked suppression represents a feedback loop that serves to shut down the PSR when a Pi substitute (As^{V}) becomes available.

Some As^{III} responses are difficult to explain in physiologic terms, yet are obvious and organized. Extensive transcriptional changes in phage-associated genes (Table 5) was too broad and operon driven to be coincidental. Expression perturbation of these genes was only encountered in the As^{III}-treated mutants, where the respective roles of PhoR and AioS appear antagonistic to one other; these mutant transcription patterns predict PhoR has repressive effects, whereas AioS plays an activating role (Table 5). One explanation could be that part of the PSR involves PhoR repression of phage proteins so as to restrict phosphate use for replicating viral genomes. Conversely, As^{III} activation of phage may be linked to oxidative stress, as recorded previously for some enterobacteria (Binnenkade *et al*., 2014). Thus, in our experimental conditions (PSR plus As^{III} exposure), these regulatory systems cancel out one another and may explain why no As^{III}-based regulatory change was observed for these and other similarly affected genes in the wild-type strain.

The discovery of AioS involvement in regulating conjugal transfer was also not anticipated, although arsenic resistance in some enterobacteria has been shown to be plasmid associated (Smith, 1978), and thus, activation of conjugal transfer genes upon As^{III} exposure could be linked in this context. In contrast, there is no PhoR influence for the conjugal transfer genes, suggesting that another regulatory function somehow balances the regulatory influence of AioS such that no net change is observed in the wild-type strain.

Another interesting wildtype strain As^{III} response concerns upregulation of genes involved in copper resistance/metabolism (Supporting Information Table 1). PhoR plays a variable role in controlling these genes (Supporting Information Table 1), but almost exclusively in cells not exposed to As^{III} (Supporting Information Table 1). At this juncture, the exact regulatory linkage is not clear except to suggest that PhoR interacts with response regulators that have both activating and repressing repressing activities. This is supported by PhoR being implicated in controlling expression of a large number of transcriptional regulators (many putative, not yet characterized; Supporting Information Table 1), perhaps indicating regulatory cascades originating from PhoR. Such entanglements with other transcriptional regulators are almost certainly involved when attempting to explain the very extensive PhoR/PSR transcriptional footprint in strain 5A as well as the observations made in similar studies with *E. coli* and *Corynebacterium glutamicum* (Ishige *et al*., 2003; Baek and Lee, 2007; Marzan and Shimizu, 2011). In the absence of As^{III}, expression of 23 putative transcriptional regulators was altered in the *phoR* mutant (Supporting Information Table 1), with each no doubt controlling their own suite of genes that then contribute to the apparent PSR. Further, there appeared to be an As^{III} effect layered on top of PhoR. In comparing As^{III}-treated *phoR* mutant and wildtype cells (Tables 1–5 and Supporting Information Table 1), relative changes could be grouped into three basic categories. The first category involves genes for which expression in $+As^{III}$ treated cells remained essentially the same as in $-As^{III}$ cells, suggesting these genes are part of the PSR *per se* and not affected by As^{III}. The second category involved expression changes (increases or decreases) that were further amplified by As^{III}, suggesting PhoR control but with an additive effect of As^{III} on top of the PSR. This may involve AioSR-based activation, which only takes effect when the cell is exposed to As^{III}, but is ultimately controlled by PhoR (Wang *et al*., 2018). A third category included genes unperturbed in $-As^{III}$ cells (i.e. no PhoR effect, *per se*), but that exhibited significantly altered transcription in $+As^{III}$ cells. Here, this could reflect de-

repression of promoters controlled by As^{III}-sensitive ArsR repressors. An example could include genes controlled by ArsR4, as its encoding gene (*arsR4*) appears to be part of PhoR/AioS circuitry (Table 2).

Reduced expression in the $-As^{III}$ treated *phoR* mutant reflects genes normally activated by PhoR-based signalling in the wild type cell and is consistent with what is most often viewed to be the role of its cognate regulator protein, PhoB; i.e., transcriptional activation via phosphorylated PhoB (PhoB-P). Conversely, genes upregulated in the $-As^{III}$ *phoR* mutant (Supporting Information Table 1) suggests genes normally repressed by PhoB-P. PhoB-P linked repression activity has been documented previously (Sola-Landa *et al*., 2008; Pratt *et al*., 2010; Santos-Beneit *et al*., 2011; Morero *et al*., 2014; Park and Kiley, 2014). Also of relevance in this regard, *phoB1* (Fig. 1) expression was not altered in $-As^{III}$ cells, whereas levels of *phoB2* (Fig. 1) were reduced ~21-fold in the *phoR* mutant. This implies that PhoB2 is likely the primary response regulator partnered to PhoR in the PSR, as opposed to PhoB1. Such a significant reduction in PhoB2 in the cell no doubt also played a role in both upregulation and downregulation.

Regarding AioS, its regulatory influence is clearly much smaller than PhoR (Fig. 2 and Supporting Information Table 1). Nevertheless, *aioS* profiling yielded interesting results that broaden our understanding of the AioS-AioR signalling system. Thus far, the regulatory role of AioS has only been linked to regulating *aioBA* when the cell is exposed to As^{III} (Kashyap *et al*., 2006; Koechler *et al*., 2010; Wang *et al*., 2018). Consistent with this view, the great majority of the transcriptional changes registered for the Δ*aioS* mutant only occurred in As^{III}-exposed cells, clearly linking this sensor kinase with primarily As^{III}-specific responses, which conforms to current expectations. Based on our recent report (Wang *et al*., 2018), positive control of *aioS* by PhoR-PhoB (Table 2) was anticipated and in turn AioS positively controls *aioB, aioA, aioC* and *aioD* (Table 2) through its interaction with its cognate response regulator AioR (Kashyap *et al*., 2006; Shi *et al*., 2017). Note that *aioX* (encodes the required periplasmic As^{III} binding protein) is controlled by PhoR (Table 2), consistent with the evidence of a Pho box associated with its promoter region (Wang *et al*., 2018), and again linking As^{III} oxidation with the PSR. AioS is also linked to the expression of genes encoding functions associated with the PSR, and its role in this regard has two opposing affects; upregulation of genes in the *pho*/*pst1* locus that is proximal to the *aio* genes (Fig. 1), but downregulation of the other, disparately located *pho*/*pst2* locus (Fig. 1 and Table 3; Supporting Information Table 1). As aforementioned, the *AioXSRBA* genes are critical for the generation of a phosphate substitute (As^{V}) under PSR conditions, and thus could also be part of a signalling system that attenuates the formal components of the PSR when a phosphate substitute (i.e. As^{V}) becomes available.

It was of interest to determine if the genes influenced by AioS might also be physically linked with σ^{54} and AioR binding sites, which are viewed to be essential for the expression of the *aioBA* genes (encode As^{III} oxidase) (Kang *et al*., 2012a; Corsini *et al*., 2017; Shi *et al*., 2018). As expected, both were found upstream of *aioB* (Supporting Information Table 2), but this was not the case for most of the genes perturbed in the *aioS* mutant (Supporting Information Table 2). Lack of association between *aioS* perturbed genes and σ^{54} and/or AioR binding sites may be due to at least two phenomena. First, there are many genes that are in As^{III}-sensitive operons known to be controlled by AioSR, but are distal from the promoter and thus could classify as an *aioS* sensitive gene not closely associated with an AioR binding site. Examples include *aioA* and *aioD*, the second and fourth genes in the *aio* operon, respectively, which are driven by the *aioB* promoter that has multiple AioR binding sites (Supporting Information Table 2). However, we draw attention to *aioC*, the third gene in this specific operon; there are two AioR binding sites and an σ^{54} binding site upstream of *aioC* (within *aioA*). This may explain the highly enhanced expression of *aioC*, although one might also expect commensurately increased *aioD* expression due to read through. However, this was not the case, though the differences may also be due to differential mRNA half-life. Some *aioS* sensitive genes have no recognizable σ^{54} or AioR binding sites, and many others have one or the other, but not both. Potentially at least, AioS may phosphorylate (an)other response regulator (i.e. crosstalk, Zhou *et al*., 2005) as we showed for PhoB1 and PhoB2 (Wang *et al*., 2018) that would then serve to regulate the expression of these genes absent of a σ^{54} and/or AioR binding site.

Advanced model

Based on the results of several studies we have conducted spanning the past decade (Kashyap *et al*., 2006; Kang *et al*., 2012a,b; 2016; Wang *et al*., 2015; 2018), we have been developing a model to visually depict and document the regulatory events occurring in strain 5A in response to As^{III} (Fig. 4). The master regulator is the PhoR-PhoB2 pair that controls the PSR, including the expression of *aioSR* (Kang *et al*., 2012b; Wang *et al*., 2018), which in turn activates *aioBA* in combination with RpoN (Kashyap *et al*., 2006; Koechler *et al*., 2010; Kang *et al*., 2012a). Expression of *aioBA* also requires the presence of As^{III}, which is the trigger ligand that interacts with the periplasmic As^{III} binding protein, AioX, that initiates the AioS-AioR transduction pathway.

Transcriptional controls are complex, occurring in a step-wise, cascade fashion. The *pho/pst2* locus encodes the actual PSR components, upregulating in response to Pi limitation. When the Pi limited cell is simultaneously exposed to As^{III}, another set of regulatory events come into play: (i) As^{III} causes ArsR1 to vacate the *phoB1* and *pstS1* promoters, which are then activated by PhoB2; (ii) PhoR phosphorylation of the resulting PhoB1 facilitates induction of *aioXSR*; and (iii) in combination with RpoN, AioR activates transcription of *aioBA*, which then transitions the cell into an As^{III} oxidizing state. We have demonstrated that both PhoR and AioS can phosphorylate PhoB1, PhoB2, as well as AioR (Wang *et al*., 2018), implying these two regulatory systems are deeply integrated. Once As^{III} oxidation begins at the cytoplasmic membrane in the periplasm, As^{V} can be taken up into cytoplasm via the PstSCAB complex, otherwise known as a high affinity phosphate (Pi) transporter. PstSCAB has higher affinity for Pi, but nevertheless will accommodate As^{V} transport when the As^{V}:Pi ratio becomes sufficiently high, which would be expected under conditions wherein Pi is already limiting so as to induce the PSR. Once inside the cell, As^{V} apparently can substitute for Pi in specific molecules (e.g. arsenolipids, functionally replacing phospholipids) resulting in enhanced growth under conditions that are limited by Pi (Wang *et al*., 2018). At this stage, feedback circuits become engaged. Specifically, PhoR-PhoB2 begin shutting down the *ars2* locus, and AioS (presumably via AioR-Pi) also begins constraining expression of the *ars2* locus. AioS-based shut down of the *pho/pst2* locus might be argued to be a second stage of the cell's response to Pi stress. As^{III} oxidation yields the phosphate analog, As^{V},

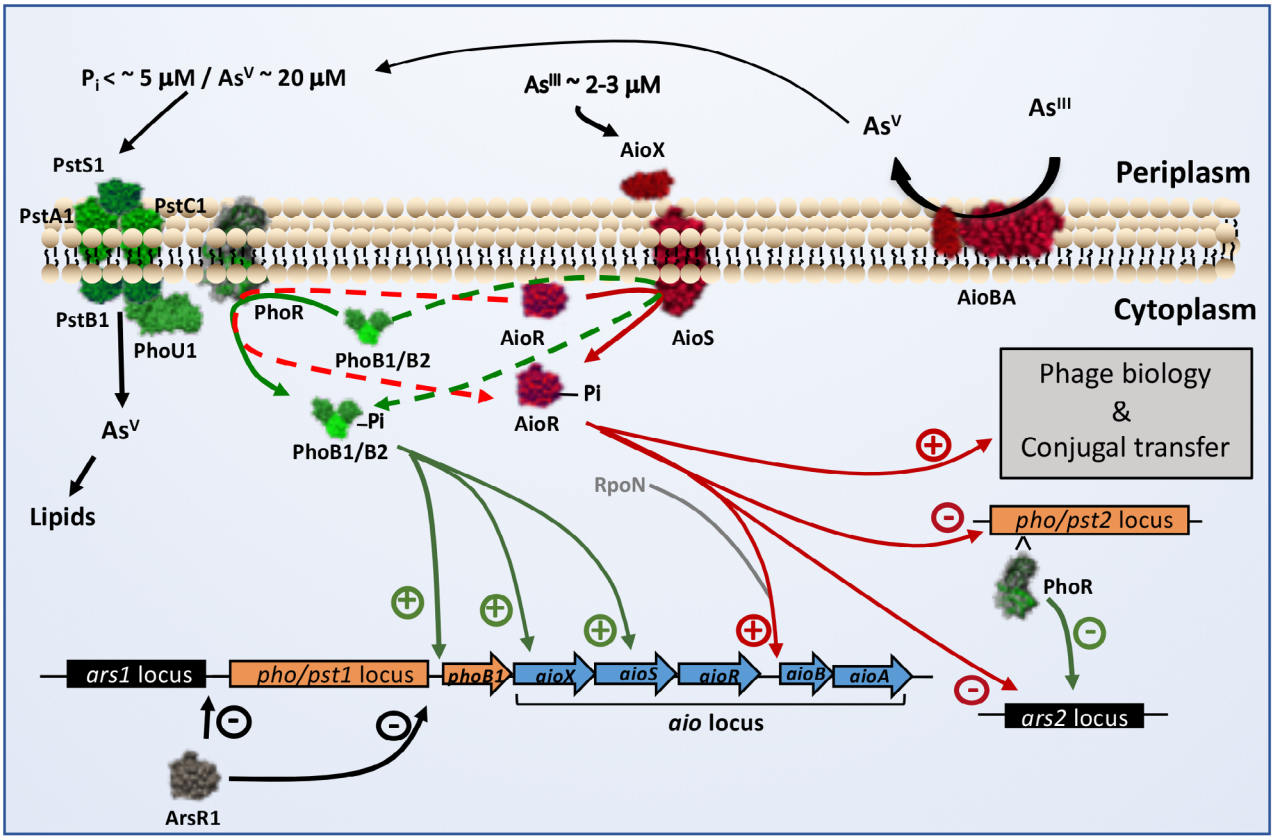

Fig. 4. Proposed model to depict the regulatory circuitry and integration of As^{III} oxidation and the PSR in *A. tumefaciens 5A,* and highlighting the role of AioS-AioR.
Vector arrows illustrate the type of regulatory activity exerted by the different regulatory proteins; (–) = negative, (+) = activation. Under conditions where As^{III} is present and environmental Pi is depleted, As^{III} enters the cell via an aquaglycerol porin (not shown) and interacts with ArsR1, causing ArsR1 to release from its DNA binding motifs that are proximal to *arsR1,* and to *pstS1* and *phoB1*, thereby opening transcription for the *arsR1, pstS1* and *phoB1* operons. The PSR signal is transduced via PhoR to the transcriptional activator PhoB1, resulting in the full induction of *phoB1* and *pstS1.* PhoB1 is also predicted to activate expression of *aioXSR,* again under the control of PhoR. With AioXSR installed, As^{III} is bound by the periplasmic AioX, which interacts with AioS to initiate the As^{III} signal transduction to the transcriptional activator AioR. Phosphorylated AioR then activates transcription of *aioBACD* in association with RpoN. The resulting As^{III} oxidation generates As^{V}, which is then taken up and can be utilized for arsenolipid synthesis sparing Pi for redistribution for critical cellular components (e.g. nucleic acids) or for essential cell functions (e.g. ATP metabolism). When intracellular Pi availability becomes enhanced, AioSR shuts down the PSR in parallel with PhoR initiating suppression of the arsenic resistance response by shutting down the *ars2* locus. Figure modified from Kang and colleagues (2012a,b) and Wang and colleagues (2018).

that selectively replaces Pi in some molecules, freeing Pi for essential cellular processes (Wang *et al*., 2018). As this sparing/replacement process begins, attenuation of the PSR ensues.

In conclusion, As^{III} exposure brings about broad changes in the model soil bacterium *A. tumefaciens* 5A. While not all bacteria will react exactly the same, it is reasonable to assume that the responses characterized herein are likely representative. As monitored at the transcriptional level, the effects are truly global, impacting metabolisms and activities central to nutrient cycling, energy generation, solute transport, iron metabolism, conjugation and phage biology. These activities are foundational to microbial activities in nature. These data confirm previously documented phenomena as well as present novel cellular changes upon As^{III} exposure, particularly highlighting the regulatory controls exerted by the sensor histidine kinases PhoR and AioS. From this we conclude that arsenic contamination of any environment would be expected to significantly alter the most basic of microbial activities, that then potentially translate into gross perturbations of all biogeochemical cycling.

Experimental procedures

Bacterial strains and growth conditions

The bacterial strains used in this study were *Agrobacterium tumefaciens* 5A (wild type) and the mutant strains 5A(Δ*aioS*), and 5A(Δ*phoR*). Briefly, the mutant strains were constructed by in-frame deletions using crossover PCR and levansucrose resistance selection of mutants as previously described (Kang *et al*., 2012b). All strains were grown at 30°C in defined minimal mannitol medium as described previously (Kang *et al*., 2012b; Wang *et al*., 2015) except the $FeCl_3$ content was reduced 10X so as not to interfere with RNA extraction and purification. This was judged to be nonlimiting because: (i) normal $FeCl_3$ levels in the minimal mannitol medium results in most being auto-oxidized to the insoluble Fe^{3+} specie and thus not bioavailable anyway (but does interfere with RNA extraction); (ii) the relative number of cells in the induction and the short duration of the experiments (maximum 6 h) cells would not result in Fe limitation; and (iii) the transcriptional response of the cells was the complete opposite of what would be expected if the cells were experiencing Fe limitation (40 of 41 affected iron-related genes were downregulated).

Overnight cultures were diluted with fresh media (0 μM phosphate) to O.D. 0.05., in quadruplicate and supplemented with either 50 μM phosphate (control) or 50 μM phosphate +100 μM As^{III} and incubated at 30°C with aeration for 6 h. Previous research has determined that induction of the *aio* genes occurs at 4 h of growth in the presence of As^{III}, and at 6 h arsenite oxidation is fully underway (Kang *et al*., 2012b). At 6 h, cells were harvested by centrifugation at 8000 x *g* for 5 min at 4°C.

Cell lysis and RNA extraction

Cell pellets were resuspended in 1 ml RNAprotect Bacteria Reagent (Qiagen) and incubated at room temperature for 5 min to stabilize cellular mRNA. Cells were then centrifuged at 5000 × *g* at 4°C for 10 min and supernatant removed. The cell pellets were resuspended in 200 μl TE buffer (10 mM Tris-Cl, 1 mM EDTA, pH 8.0) containing 1 mg/ml lysozyme (ThermoScientific) and mixed by pipetting for 5 min to lyse cells. Following lysis, RNA was extracted using an RNeasy® Mini Kit (Qiagen), including on-column DNase digestion (verified to be DNA free via PCR). RNA concentration was measured using a SpectraMax microtiter plate reader (Molecular Devices, CA). RNA was further purified using the RNA Cleanup protocol included in the RNeasy® Mini Kit (Qiagen), with the final concentration and purity confirmed using an Agilent 2100 Bioanalyzer (Agilent Technologies).

Library preparation and RNA sequencing

RNA was sequenced at the Brigham Young University DNA Sequencing Center (Provo, UT), employing their in-house pipeline protocols. Briefly, ribosomal RNA was removed using the Illumina Ribo-Zero rRNA Removal Kit for Gram-negative bacteria. Resulting RNA was prepped for sequencing using the Illumina TruSeq Stranded Total RNA Sample Prep. The cDNA library was sequenced in high output mode using Illumina sequencing technology (Illumina HiSeq 2500 sequencing platform), generating 50 bp single-stranded reads, with at least 12 million reads per sample. All reads have been submitted to the NCBI Sequence Read Archive (accession number PRJNA494424).

Data processing and analysis

Raw sequences were first assessed for quality using FastQC (Version 0.11.4; Andrews, 2010). All sequences had high quality scores (> than 30). Ribosomal RNA and adapter sequences were removed using Trimmomatic (Version 0.32) (Bolger *et al*., 2014). Sequences were then aligned and quantified using Kallisto (Version 0.43) (Bray *et al*., 2016). The parameters used for alignment were kmer size of 31, fragment length 180 and standard deviation of 20, using the EnsemblBacteria genome for *Agrobacterium tumefaciens* 5A (ASM23612v2). Kallisto also performed 100 bootstraps for assessment of technical variance. After alignment and quantification, the R package 'Sleuth' was used for differential analysis. Sleuth uses the bootstraps performed in Kallisto to adjust for

technical variance as well as compare groups of samples using the Wald Test. *p* Values were adjusted for multiple comparisons using the Benjamini–Hochberg method (Benjamini and Hochberg, 1995). Reads were normalized to transcripts per kilobase million (TPM), which were obtained by dividing transcript number by the length of gene in kilobases, resulting in reads per kilobase. All reads per kilobase were counted within a sample and that number was divided by 1 million for a per million scaling factor to generate the TPM. Only differentially expressed genes with an average TPM > 1, a fold change greater than ± 2 and a *q* value less than 0.05 were included in the analysis. Gene IDs were converted using Uniprot to access available E.C. numbers, gene ontology terms and gene names.

Motif searches

To search for putative σ^{54} (RpoN) and AioR binding sites, 300 nucleotides upstream of genes differentially regulated in the *aioS* mutant (153 genes) were scanned using the Find Individual Motif Occurrence algorithm in MEME Suite (5.0.1). FIMO utilizes log-posterior odds scoring and position-specific priors to search for a given motif (Grant *et al*., 2011; Cuellar-Partida *et al*., 2012). The well-defined σ^{54} consensus sequence, TGG(N9)TGC, (Cannon *et al*., 1993; Kang *et al*., 2012a) and proposed AioR binding sequences GTCCGCAAAATCAGGACA (Corsini *et al*., 2017) and GT[TC][AC][CG][GCT][AG][AG]A[ACT][CGA][GCT][GTA]AAC (Shi *et al*., 2018) were used as search inputs. Only motifs with a *p* value ≤0.001 were considered as putative binding sites. Representative sequence logos were constructed using WebLogo (2.8.2, Berkley, CA).

Acknowledgements

Funding for this research was provided by the National Science Foundation Systems and Synthetic Biology program (MCB-1413321, MCB-1714556): TRM was also supported by the Montana Agricultural Experiment Station (911310). BB was additionally supported by Montana INBRE (NIH P20GM103474). We thank Tara Saley and Savanna Stendahl for their contributions to this work.

References

Agency for Toxic Substances and Disease Registry (2017) *Priority Substance List* (US Department of Health and Human Services).

Andres, J., Arsène-Ploetze, F., Barbe, V., Brochier-Armanet, C., Cleiss-Arnold, J., Coppée, J.Y., *et al*. (2013) Life in an arsenic-containing gold mine: genome and physiology of the autotrophic arsenite-oxidizing bacterium *Rhizobium* sp. NT-26. *Genome Biol Evol* **5**: 934–953.

Andrews, S. (2010) A quality control tool for high throughput sequence data. www.bioinformatics.babraham.ac.uk/projects/fastqc.

Baek, J.H., and Lee, S.Y. (2007) Transcriptome Analysis of Phosphate Starvation Response in Escherichia coli, *J Microbiol Biotechnol* **17**: 244–252.

Benjamini, Y., and Hochberg, Y. (1995) Controlling the false discovery rate : a practical and powerful approach to multiple testing. *J R Statist Soc* **57**: 289–300.

Binnenkade, L., Teichmann, L., and Thormann, K.M. (2014) Iron triggers λSo prophage induction and release of extracellular DNA in *Shewanella oneidensis* MR-1 biofilms. *Appl Environ Microbiol* **80**: 5304–5316.

Bolger, A.M., Lohse, M., and Usadel, B. (2014) Trimmomatic: a flexible trimmer for illumina sequence data. *Bioinformatics* **30**: 2114–2120.

Bray, N.L., Pimentel, H., Melsted, P., and Pachter, L. (2016) Near-optimal probabilistic RNA-seq quantification. *Nat Biotechnol* **34**: 525–527.

Cannon, W., Claverie-Martin, F., Austin, S., and Buck, M. (1993) Core RNA polymerase assists binding of the transcription factor sigma54 to promoter DNA. *Mol Microbiol* **8**: 287–298.

Cleiss-Arnold, J., Koechler, S., Proux, C., Fardeau, M.-L., Dillies, M.-A., Coppee, J.-Y., *et al*. (2010) Temporal transcriptomic response during arsenic stress in *Herminiimonas arsenicoxydans*. *BMC Genomics* **11**: 709.

Corsini, P.M., Walker, K.T., and Santini, J.M. (2017) Expression of the arsenite oxidation regulatory operon in *Rhizobium* sp. str. NT-26 is under the control of two promoters that respond to different environmental cues. *Microbiologyopen* **7**: 1–8.

Cuellar-Partida, G., Buske, F.A., McLeay, R.C., Whitington, T., Noble, W.S., and Bailey, T.L. (2012) Epigenetic priors for identifying active transcription factor binding sites. *Bioinformatics* **28**: 56–62.

Grant, C.E., Bailey, T.L., and Noble, W.S. (2011) FIMO: scanning for occurrences of a given motif. *Bioinformatics* **27**: 1017–1018.

Hao, X., Lin, Y., Johnstone, L., Liu, G., Wang, G., Wei, G., *et al*. (2012) Genome sequence of the arsenite-oxidizing strain *Agrobacterium tumefaciens* 5A. *J Bacteriol* **194**: 903.

Hsieh, Y., and Wanner, B. (2010) Global regulation by the seven-component Pi signaling system. *Curr Opin Microbiol* **13**: 198–203.

Imlay, J.A. (2013) The molecular mechanisms and physiological consequences of oxidative stress: lessons from a model bacterium. *Nat Rev Microbiol* **11**: 443–454.

Inskeep, W.P., McDermott, T.R., and Fendorf, S. (2001) Arsenic (V)/(III) cycling in soils and natural waters: chemical and microbiological processes . In *Environmental Chemistry of Arsenic*, Frankenberger, W.F., and Macy, J. M. (eds). New York: Marcell Dekker, pp. 183–215.

Ishige, T., Krause, M., Bott, M., Wendisch, V.F., and Sahm, H. (2003) The phosphate starvation stimulon of *Corynebacterium glutamicum* determined by DNA microarray analyses. *J Bacteriol* **185**: 4519–4529.

Kang, Y.-S., Bothner, B., Rensing, C., and McDermott, T.R. (2012a) Involvement of RpoN in regulating bacterial arsenite oxidation. *Appl Environ Microbiol* **78**: 5638–5645.

Kang, Y.S., Heinemann, J., Bothner, B., Rensing, C., and McDermott, T.R. (2012b) Integrated co-regulation of

bacterial arsenic and phosphorus metabolisms. *Environ Microbiol* **14**: 3097–3109.
Kang, Y.-S., Shi, Z., Bothner, B., Wang, G., and McDermott, T.R. (2015) Involvement of the Acr3 and DctA anti-porters in arsenite oxidation in *Agrobacterium tumefaciens* 5A. *Environ Microbiol* **17**: 1950–1962.
Kang, Y.S., Brame, K., Jetter, J., Bothner, B.B., Wang, G., Thiyagarajan, S., and McDermott, T.R. (2016) Regulatory activities of four ArsR proteins in *Agrobacterium tumefaciens* 5A. *Appl Environ Microbiol* **82**: 3471–3480.
Kapaj, S., Peterson, H., Liber, K., and Bhattacharya, P. (2006) Human health effects from chronic arsenic poisoning—a review. *J Environ Sci Health A* **41**: 2399–2428.
Kashyap, D.R., Botero, L.M., Franck, W.L., Hassett, D.J., and McDermott, T.R. (2006) Complex regulation of arsenite oxidation in *Agrobacterium tumefaciens*. *J Bacteriol* **188**: 1081–1088.
Koechler, S., Cleiss-Arnold, J., Proux, C., Sismeiro, O., Dillies, M.-A., Goulhen-Chollet, F., *et al*. (2010) Multiple controls affect arsenite oxidase gene expression in *Herminiimonas arsenicoxydans*. *BMC Microbiol* **10**: 53.
Li, H., Li, M., Huang, Y., Rensing, C., and Wang, G. (2013) In silico analysis of bacterial arsenic islands reveals remarkable synteny and functional relatedness between arsenate and phosphate. *Front Microbiol* **4**: 1–10.
Liu, G., Liu, M., Kim, E.-H., Maaty, W.S., Bothner, B., Lei, B., *et al*. (2012) A periplasmic arsenite-binding protein involved in regulating arsenite oxidation. *Environ Microbiol* **14**: 1624–1634.
Marzan, L.W., and Shimizu, K. (2011) Metabolic regulation of *Escherichia coli* and its phoB and phoR genes knockout mutants under phosphate and nitrogen limitations as well as at acidic condition. *Microb Cell Fact* **10**: 39–15.
Morero, N.R., Botti, H., Nitta, K.R., Carrión, F., Obal, G., Picardeau, M., and Buschiazzo, A. (2014) HemR is an OmpR/PhoB-like response regulator from Leptospira, which simultaneously effects transcriptional activation and repression of key haem metabolism genes. *Mol Microbiol* **94**: 340–352.
Naujokas, M.F., Anderson, B., Ahsan, H., Aposhian, H.V., Graziano, J.H., Thompson, C., and Suk, W.A. (2013) The broad scope of health effects from chronic arsenic exposure: update on a worldwide public health problem. *Environ Health Perspect* **121**: 295–302.
Park, D.M., and Kiley, P.J. (2014) The influence of repressor DNA binding site architecture on transcriptional control. *MBio* **5**: 1–11.
Parvatiyar, K., Alsabbagh, E.M., Ochsner, U., Stegemeyer, M., Smulian, A.G., Hwang, S.H., *et al*. (2005) Global analysis of cellular factors and responses involved in *Pseudomonas aeruginosa* resistance to arsenite. *J Bacteriol* **187**: 4853–4864.
Pratt, J.T., Ismail, A.M., and Camilli, A. (2010) PhoB regulates both environmental and virulence gene expression in *Vibrio cholerae*. *Mol Microbiol* **77**: 1595–1605.
Santos-Beneit, F., Barriuso-Iglesias, M., Fernández-Martínez, L.T., Martínez-Castro, M., Sola-Landa, A., Rodríguez-García, A., and Martín, J.F. (2011) The RNA polymerase omega factor rpoZ is regulated by phop and has an important role in antibiotic biosynthesis and morphological differentiation in *Streptomyces coelicolor*. *Appl Environ Microbiol* **77**: 7586–7594.
Shi, K., Fan, X., Qiao, Z., Han, Y., McDermott, T.R., Wang, Q., and Wang, G. (2017) Arsenite oxidation regulator AioR regulates bacterial chemotaxis towards arsenite in *Agrobacterium tumefaciens* GW4. *Sci Rep* **7**: 43252.
Shi, K., Wang, Q., Fan, X., and Wang, G. (2018) Proteomics and genetic analyses reveal the effects of arsenite oxidation on metabolic pathways and the roles of AioR in *Agrobacterium tumefaciens* GW4. *Environ Pollut* **235**: 700–709.
Smith, W.H. (1978) Arsenic resistance in Enterobacteria : its transmission by conjugation and by phage. *J Gen Microbiol* **109**: 49–56.
Sola-Landa, A., Rodríguez-García, A., Apel, A.K., and Martín, J.F. (2008) Target genes and structure of the direct repeats in the DNA-binding sequences of the response regulator PhoP in *Streptomyces coelicolor*. *Nucleic Acids Res* **36**: 1358–1368.
Wang, Q., Kang, Y.S., Alowaifeer, A., Shi, K., Fan, X., Wang, L., *et al*. (2018) Phosphate starvation response controls genes required to synthesize the phosphate analog arsenate. *Environ Microbiol* **20**: 1782–1793.
Wang, Q., Qin, D., Zhang, S., Wang, L., Li, J., Rensing, C., *et al*. (2015) Fate of arsenate following arsenite oxidation in *Agrobacterium tumefaciens* GW4. *Environ Microbiol* **17**: 1926–1940.
Wanner, B.L. (1993) Gene regulation by phosphate in enteric bacteria. *J Cell Biochem* **51**: 47–54.
Wanner, B.L. (1996) Phosphorus assimilation and control of the phosphate regulon *Escherichia coli Salmonella*. *Cell Mol Biol* **1**: 1357–1381.
Wanner, B.L., and Chang, B.D. (1987) The phoBR operon in *Escherichia coli* K-12. *J Bacteriol* **169**: 5569–5574.
Zhou, L., Grégori, G., Blackman, J.M., Robinson, J.P., and Wanner, B.L. (2005) Stochastic activation of the response regulator PhoB by noncognate histidine kinases. *J Integr Bioinform* **2**: 111–124.

Supporting Information

Additional Supporting Information may be found in the online version of this article at the publisher's web-site:

Table S1 Complete summary listing of gene expression changes as a result of As(III) exposure and/or ▽*phoR* and ▽*aioS* mutations. All fold-changes shown are statistically significant as described in Experimental Procedures. Genes are arranged according to functional categories. Lack of fold change indicates expression changes did not meet the base criteria of (±) twofold change and p value < 0.05. *TPM average for one treatment group < 1.

Table S2. Summary listing of all genes perturbed by the *aioS* mutation and those that are associated with a putative RpoN binding site and or a putative AioR binding site (within 300 nt upstream of translational start site). The RpoN search motif is shown on the left and the AioR search motifs are as shown on the right. 'S' indicates AioR sequence from Shi and colleagues (2017); 'C' indicates AioR sequence from Corsini and colleagues (2017). Lack of fold change indicates expression changes did not meet the base criteria of (±) twofold change and p value < 0.05.